

Collision of ϕ^4 kinks free of the Peierls–Nabarro barrier in the regime of strong discreteness

Alidad Askari,^{1,*} Aliakbar Moradi Marjaneh,^{2,†} Zhanna G. Rakhmatullina,^{3,‡}
Mahdy Ebrahimi-Loushab,^{4,§} Danial Saadatmand,^{5,¶} Vakhid A. Gani,^{6,7,**}
Panayotis G. Kevrekidis,^{8,9,††} and Sergey V. Dmitriev^{10,11,‡‡}

¹*Department of Physics, Faculty of Science,
University of Hormozgan, P.O.Box 3995, Bandar Abbas, Iran*

²*Young Researchers and Elite Club, Quchan Branch,
Islamic Azad University, Quchan, Iran*

³*Institute for Metals Superplasticity Problems,
Russian Academy of Sciences, Ufa 450001, Russia*

⁴*Quchan Technical and Vocational University of Iran, Quchan, Iran*

⁵*Department of Physics, University of Sistan and Baluchestan, Zahedan, Iran*

⁶*Department of Mathematics, National Research Nuclear University
MEPhI (Moscow Engineering Physics Institute), Moscow 115409, Russia*

⁷*Theory Department, Institute for Theoretical and Experimental Physics of
National Research Centre “Kurchatov Institute”, Moscow 117218, Russia*

⁸*Department of Mathematics and Statics,
University of Massachusetts, Amherst, Massachusetts 01003, USA*

⁹*Mathematical Institute, University of Oxford, OX26GG, UK*

¹⁰*Institute of Molecule and Crystal Physics,
Ufa Federal Research Center of Russian Academy of Sciences, Ufa 450075, Russia*

¹¹*National Research Tomsk State University,
Lenin Avenue 36, 634050 Tomsk, Russia*

Abstract

The two major effects observed in collisions of the *continuum* ϕ^4 kinks are (i) the existence of critical collision velocity v_c above which the kinks always emerge from the collision and (ii) the existence of the escape windows for multi-bounce collisions with the velocity below v_c , associated with the energy exchange between the kink's internal and translational modes. The potential merger (for sufficiently low collision speeds) of the kink and antikink produces a bion with oscillation frequency ω_B , which constantly radiates energy, since its higher harmonics are always within the phonon spectrum. Similar effects have been observed in the discrete ϕ^4 kink-antikink collisions for relatively weak discreteness. Here we analyze kink-antikink collisions in the regime of strong discreteness considering an exceptional discretization of the ϕ^4 field equation where the static Peierls–Nabarro potential is precisely zero and the not-too-fast kinks can propagate practically radiating no energy. Several new effects are observed in this case, originating from the fact that the phonon band width is small for strongly discrete lattices and for even higher discreteness an inversion of the phonon spectrum takes place with the short waves becoming low-frequency waves. When the phonon band is narrow, not a bion but a discrete breather with frequency ω_{DB} and all higher harmonics being outside the phonon band is formed. When the phonon spectrum is inverted, the kink and antikink become mutually repulsive solitary waves with oscillatory tails, and their collision is possible only for velocities above a threshold value sufficient to overcome their repulsion.

PACS numbers: 11.10.Lm, 11.27.+d, 05.45.Yv, 03.50.-z

* alidadaskari@gmail.com

† Corresponding Author: moradimarjaneh@gmail.com

‡ rakhzha@gmail.com

§ ebrahimi.mahdy@gmail.com

¶ saadatmand.d@gmail.com

** vagani@mephi.ru

†† kevrekid@umass.edu

‡‡ dmitriev.sergey.v@gmail.com

I. INTRODUCTION

Continuum and discrete Klein–Gordon type equations contribute to understanding of many physical phenomena [1–4]. In discrete models the Lorentz invariance is lost and several new important effects are observed, such as for example, the appearance of the Peierls–Nabarro potential, the associated reduction of soliton mobility, the radiation produced by moving solitary waves, etc. [2–6]. The case of strong discreteness is of particular interest and it is encountered in many applications, for example, in the description of arrays of Josephson junctions [7], dissipative nonlinear discrete systems [8], dynamics of crowdions [9–13] and dislocations [14–16] in crystals, propagation of domain walls in magnetic materials [17], motion of spring-mass chains [18], in the discussion of electric charge transport in molecular chains [19]. The consideration of the strongly discrete (anti-continuum) limit is a well-known approach aiming towards the analytical treatment of discrete breathers [20, 21].

One particularly central problem in the dynamics of solitary waves is the analysis of their collision outcomes, especially beyond the merely-phase-shifting elastic wave interactions within integrable models [22–39]. Continuum Klein–Gordon equations, apart from the famous integrable sine-Gordon example [4], support exact solutions in the form of moving kinks which interact inelastically. Collisions between a kink and an antikink moving towards each other with initial velocities $\pm v_c$ have been extensively studied. It has been found that if $v_c > v^*$, where v^* is a critical collision velocity, then the kink and antikink separate after the first collision [22–24, 26–28]. On the other hand, collisions with $v_c < v^*$ produce a set of escape windows having fractal structure [24, 26–28]. When the collision velocity is within such a window, the kink and antikink move away from each other after multiple collisions. The kinks’ internal vibrational modes [40] have been extensively argued to be responsible for this effect: they store some energy of the kinks’ translational motion which can return back in the subsequent collisions and the kink and antikink overcome mutual attraction. If the kink and antikink do not split after a few collisions, they lose a substantial amount of energy to small amplitude radiative wavepackets (emitted from the collision location) and, being unable to overcome the mutual attraction, create a bound oscillatory state called bion, whose main frequency lies below the phonon band but higher harmonics within the band. Resonating with the phonons, the bion constantly radiates energy and its amplitude gradually decreases.

The effect of weak discreteness on the solitary wave collisions was studied in [26, 29] and radiationless energy exchange between colliding quasi-particles was described. On the other hand, the collision of solitary waves in strongly discrete Klein–Gordon systems has not been studied so far. The reason is the above mentioned immobility of kinks in the presence of Peierls–Nabarro potential induced by discreteness. However this difficulty can be overcome by considering exceptional discretizations [41] of the Klein–Gordon equations where the static Peierls–Nabarro potential is precisely zero [41–53]. In the work [54], kink-antikink collisions have been analyzed in various models free of the static Peierls–Nabarro potential for the case of weak discreteness (lattice spacing $h \sim 0.1$). It has been found that collisions become more elastic with increasing h because the critical collision velocity v^* , above which kinks separate after the first collision, reduces for larger h .

In the present work, for the ϕ^4 equation discretized according to the method proposed in [42, 43], we analyze kink-antikink collisions in the regime of strong discreteness ($h \sim 1$) in the absence of the static Peierls–Nabarro potential. We find that this setting is conducive to the emergence of multiple new features including the formation of persistent discrete breathers (rather than bions) in the strongly discrete regime. Another key finding is the potential fundamental modification of the nature of the interaction from an attractive to a repulsive one upon the inversion of the phonon band for strong discreteness in such models.

Our presentation is structured as follows. In section II we present the (exceptional discretization) models and some of their principal static properties. Then in section III we examine the collisions of kinks and antikinks in them. Finally, in section IV we summarize our findings and present our conclusions, as well as some challenges for future work.

II. THE ϕ^4 FIELD AND ITS EXCEPTIONAL DISCRETIZATION

A. Continuum ϕ^4 equation and its conventional discretization

The Klein–Gordon field-theoretic model can be defined by the Hamiltonian

$$H = \int_{-\infty}^{+\infty} \left[\frac{1}{2} \phi_t^2 + \frac{1}{2} \phi_x^2 + V(\phi) \right] dx, \quad (1)$$

where $\phi(x, t)$ is a real scalar function of spatial and temporal coordinates x and t , respectively. The subscripts x and t denote differentiation with respect to the corresponding

coordinate. The function $V(\phi)$ defines the on-site potential, which for the ϕ^4 model looks like

$$V(\phi) = \frac{1}{2} (1 - \phi^2)^2. \quad (2)$$

The Hamiltonian (1) with the potential (2) gives the following equation of motion:

$$\phi_{tt} - \phi_{xx} - 2\phi(1 - \phi^2) = 0. \quad (3)$$

This equation has an exact solution in the form of a moving kink (antikink),

$$\phi = \pm \tanh \frac{x - x_0 - vt}{\sqrt{1 - v^2}}, \quad (4)$$

for the upper (lower) sign, which propagates with the velocity v starting at $t = 0$ from the initial position $x = x_0$.

The discrete ϕ^4 equation is introduced on the lattice $x = nh$ having the lattice spacing $h > 0$, where n is integer. The conventional discretization of the ϕ^4 equation (3) reads [22]:

$$\ddot{\phi}_n = \frac{1}{h^2} (\phi_{n-1} - 2\phi_n + \phi_{n+1}) + 2\phi_n (1 - \phi_n^2), \quad (5)$$

where $\phi_n(t) = \phi(nh, t)$ and differentiation with respect to time is denoted by overdot. This discretization conserves the following Hamiltonian:

$$H = \frac{h}{2} \sum_n \left[\dot{\phi}_n^2 + \left(\frac{\phi_{n+1} - \phi_n}{h} \right)^2 + (1 - \phi_n^2)^2 \right]. \quad (6)$$

Collision of highly discrete kinks cannot be studied within this model because the kinks are trapped by the Peierls–Nabarro potential and cannot propagate freely.

B. Exceptional discretization of the ϕ^4 equation

Speight has derived the following discrete ϕ^4 model [42, 43]:

$$\begin{aligned} \ddot{\phi}_n &= \left(\frac{1}{h^2} + \frac{1}{3} \right) (\phi_{n-1} - 2\phi_n + \phi_{n+1}) \\ &+ 2\phi_n - \frac{1}{9} \left[2\phi_n^3 + (\phi_n + \phi_{n-1})^3 + (\phi_n + \phi_{n+1})^3 \right] \equiv f_n, \end{aligned} \quad (7)$$

which possesses the Hamiltonian

$$H = \frac{h}{2} \sum_n \left(\dot{\phi}_n^2 + u^2 \right), \quad (8)$$

where

$$u \equiv \pm \frac{\phi_n - \phi_{n-1}}{h} - 1 + \frac{\phi_{n-1}^2 + \phi_{n-1}\phi_n + \phi_n^2}{3}. \quad (9)$$

For equilibrium states, we have that $u = 0$, which can be used for obtaining the kink profile (see below). Note that we have denoted the right-hand side of Eq. (7) as f_n , which is the force acting on n -th site.

It can be proved [42, 43] that static kinks of the model (7) can be derived iteratively from the two-point map of setting (9) equal to 0, which is quadratic algebraic equation having the roots

$$\phi_{n\pm 1} = -\frac{\phi_n}{2} \mp \frac{3}{2h} \pm \frac{\sqrt{3}}{2} \sqrt{-\phi_n^2 \pm \frac{6}{h}\phi_n + \frac{3}{h^2} + 4}. \quad (10)$$

One can take in Eq. (10) either the upper or the lower signs. The iterations can be started from any initial value $|\phi_n| < 1$ to produce a static kink placed arbitrarily with respect to the lattice. The on-site kink is found for $\phi_n = 0$ and the inter-site kink for $\phi_n = 3/h - \sqrt{3 + 9/h^2}$. All such kinks have exactly the same potential energy and thus they do not experience a static Peierls–Nabarro potential.

Examples of the inter-site static kink profiles, constructed by iterating Eq. (10), are shown in Fig. 1(a) for $h = 0.5$ by dots and $h = 1.5$ by rhombuses. Note that for $h < 1$ kink's tails are monotonic, while for $h > 1$ they oscillate around the asymptotics ± 1 . The latter will play a key role in the modified interaction of the kink and antikink for $h > 1$, as we will show below.

C. Spectrum of vacuum and small-amplitude vibrations localized on the kink

Let ϕ_n^0 be an equilibrium static solution of Eq. (7). Small-amplitude oscillations around this solution can be studied by inserting $\phi_n(t) = \phi_n^0 + \varepsilon_n(t)$ into the equation of motion (7), where $\varepsilon_n \ll 1$, and obtaining the linearized equation in the form

$$\begin{aligned} \ddot{\varepsilon}_n = & \frac{1}{h^2} (\varepsilon_{n-1} - 2\varepsilon_n + \varepsilon_{n+1}) + \frac{1}{3} \left[1 - (\phi_n^0 + \phi_{n-1}^0)^2 \right] \varepsilon_{n-1} \\ & + \frac{1}{3} \left[1 - (\phi_n^0 + \phi_{n+1}^0)^2 \right] \varepsilon_{n+1} + \frac{1}{3} \left[4 - 2(\phi_n^0)^2 - (\phi_n^0 + \phi_{n-1}^0)^2 - (\phi_n^0 + \phi_{n+1}^0)^2 \right] \varepsilon_n. \end{aligned} \quad (11)$$

Substituting into Eq. (11) the ansatz $\varepsilon_n = \exp(iqn - i\omega t)$, where ω is the frequency and q is the wave number, one obtains the eigenvalue problem for finding the spectrum of small-amplitude vibrations around the static solution ϕ_n^0 .

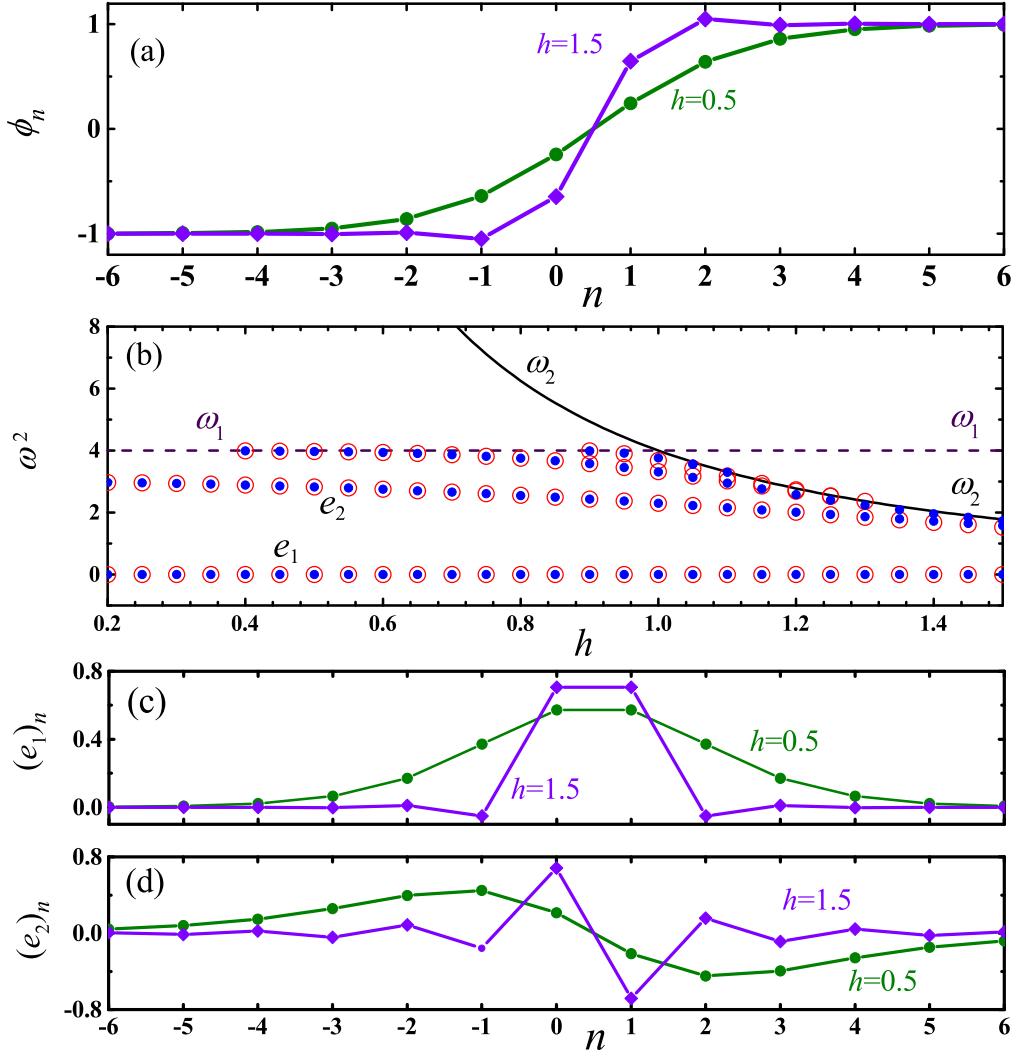


FIG. 1. (a) Inter-site static kink profiles for $h = 0.5$ (dots) and $h = 1.5$ (rhombuses). For $h < 1$ the kink's tails are monotonic, while for $h > 1$ they oscillate around the asymptotics ± 1 . (b) Borders of the phonon spectrum, ω_1 and ω_2 , as the functions of h , shown by the dashed and solid lines, respectively. The lines cross at $h = 1$. The scattered data shows the frequencies of the small-amplitude vibrational modes localized on the on-site (dots) and inter-site (circles) static kinks. The zero-frequency mode e_1 is the Goldstone translational mode, which is used for kink boosting. The second lowest frequency mode e_2 is the kink's internal mode. (c), (d) Profiles of the Goldstone translational mode and kink's internal mode, respectively, for the kinks shown in (a).

In particular, the spectrum of vacuum solution $\phi_n^0 = \pm 1$ is

$$\omega^2 = 4 + 4 \frac{1 - h^2}{h^2} \sin^2 \left(\frac{q}{2} \right). \quad (12)$$

This spectrum lies in between

$$\omega_1^2 = 4 \quad \text{and} \quad \omega_2^2 = 4 + 4 \frac{1 - h^2}{h^2}. \quad (13)$$

At $h = 1$ one has $\omega_1 = \omega_2$, i.e., the width of the spectrum vanishes and hence linear modes arise at a single frequency, namely $\omega = 2$. This situation where the frequency is independent of wavenumber is referred to as a flat band and is of particular interest in recent studies [55]. For $h < 1$ the short waves ($|q| \approx \pi$) have frequencies higher than the long waves ($|q| \approx 0$). For $h > 1$ the situation is opposite.

For the static kink solution ϕ_n^0 the eigenvalue problem is solved numerically. For this, a kink is placed in the middle of the lattice of $N = 200$ particles with boundary conditions $\phi_1 = -1$, $\phi_N = 1$. The solution of the eigenvalue problem gives $N - 2$ eigenfrequencies ω_k and the same number of eigenvectors, $(e_k)_n$. Most of the eigenfrequencies lie within the phonon spectrum of vacuum but a few of them are below the phonon spectrum. This is demonstrated in Fig. 1(b). The borders of the phonon spectrum as the functions of h , Eq. (13), are shown by the dashed and solid lines. Dots and circles indicate frequencies of the modes localized on the on-site and inter-site kink, respectively. For any h there exists the zero frequency mode e_1 , which is the translational (Goldstone) mode. The mode e_2 , which has the lowest non-zero frequency, is nothing but the kink's internal mode, which in the continuum limit ($h \rightarrow 0$) has frequency $\sqrt{3}$. In Fig. 1(c) we plot the Goldstone modes and in Fig. 1(d) the kink's internal modes for the inter-site kinks shown in (a), i.e., for the discreteness parameter $h = 0.5$ (dots) and $h = 1.5$ (rhombuses).

D. Interaction of well separated kink and antikink

For further discussion it is instructive to understand how the kink and antikink interact with each other at large distances and how this interaction depends on the lattice spacing h . In the continuum models, the force acting between the kinks is usually calculated as the negative of the slope of the potential energy of their interaction. In the regime of strong discreteness ($h \sim 1$), the kink is localized on a few particles. Using this fact, we just calculate

the force acting on the central particle of the on-site kink from the tail of an on-site antikink, which is located at some distance to the right of the kink, see Fig. 2(a). High symmetry of the considered structure allows to solve the problem. The calculation will be done in the adiabatic approximation assuming that the kink and the antikink are at rest. Let ϕ_n^0 is the static kink solution and ϕ_n^t is the antikink tail. The tail solution we take in the form

$$\phi_n^t = 1 + \epsilon_n^t, \quad (14)$$

where $|\epsilon_n^t| \ll 1$. The force acting on the n -th site, which is within the kink, can be calculated by substituting the linear superposition $\phi_n = \phi_n^0 + \epsilon_n^t$ into the static version of Eq. (7) and linearizing with respect to ϵ_n^t . The result is

$$\begin{aligned} f_n = & \frac{1}{h^2} (\epsilon_{n-1}^t - 2\epsilon_n^t + \epsilon_{n+1}^t) + \frac{1}{3} \left[1 - (\phi_n^0 + \phi_{n-1}^0)^2 \right] \epsilon_{n-1}^t \frac{1}{3} \left[1 - (\phi_n^0 + \phi_{n+1}^0)^2 \right] \epsilon_{n+1}^t \\ & + \frac{1}{3} \left[4 - 2(\phi_n^0)^2 - (\phi_n^0 + \phi_{n-1}^0)^2 - (\phi_n^0 + \phi_{n+1}^0)^2 \right] \epsilon_n^t. \end{aligned} \quad (15)$$

Notice that linear combination of the kink solution and the antikink tail solution considered here can be used for kinks with short-range tails, as in our case, but this approximation may not work for kinks with long-range tails, see, e.g., [39, 56–59].

An approximate kink tail solution can be derived by substituting Eq. (14) into Eq. (10) and linearizing with respect to ϵ_n^t . The resulting iterative formula reads

$$\epsilon_{n\pm 1}^t = \frac{1 \mp h}{1 \pm h} \epsilon_n^t, \quad (16)$$

where one can take either upper or lower signs. It can be seen from Eq. (16) that for $h < 1$ all ϵ_n^t have the same sign, so that the kink's tail monotonously approaches the value $\phi_n = 1$. For $h > 1$ the tail oscillates near $\phi_n = 1$ since ϵ_n^t and $\epsilon_{n\pm 1}^t$ have opposite signs. Note that the antikink tail is a mirror image of the kink tail (16), that is why the antikink tail can be written as

$$\epsilon_{n\pm 1}^t = \frac{1 \pm h}{1 \mp h} \epsilon_n^t. \quad (17)$$

The force f_n acting on any site within the kink can be now calculated for any given value of $\epsilon_n^t \ll 1$ after finding $\epsilon_{n\pm 1}^t$ from Eq. (17) and substituting into Eq. (15). Recall that the static kink solution can be found iteratively for any given $-1 < \phi_n^0 < 1$ from Eq. (10).

The analytical expression for the force f_n can be simplified for the case of highly symmetric on-site kink. Let the on-site kink is located at $n = n_0$, i.e., $\phi_{n_0}^0 = 0$. Then from Eq. (10) one

finds the displacements for the neighboring sites:

$$\phi_{n_0 \pm 1}^0 = \mp \frac{3}{2h} \pm \frac{\sqrt{3}}{2} \sqrt{\frac{3}{h^2} + 4}. \quad (18)$$

For a given small value $\epsilon_{n_0}^t$ we find $\epsilon_{n_0 \pm 1}^t$ from Eq. (17) and substituting these values together with $\phi_{n_0}^0 = 0$ and $\phi_{n_0+1} = -\phi_{n_0-1}$ into Eq. (15), we obtain the force acting from the antikink's tail on the central particle of the on-site kink:

$$f_{n_0} = -\frac{4\epsilon_{n_0}^t}{(1-h)(1+h)} - \frac{\epsilon_{n_0}^t}{3} \left\{ \frac{2(1+h^2)}{(1-h)(1+h)} \left[1 - (\phi_{n_0+1}^0)^2 \right] - 2(\phi_{n_0+1}^0)^2 + 4 \right\}, \quad (19)$$

where ϕ_{n_0+1} is given by Eq. (18).

From Eq. (19) it can be seen that f_{n_0} is proportional to $\epsilon_{n_0}^t$. The dependence of $f_{n_0}/\epsilon_{n_0}^t$ on h is shown in Fig. 2(b). It is interesting to note that the sign of the force changes at $h = 1$ so that the kink and antikink attract each other for $h < 1$ and repel each other for $h > 1$. This fact will be confirmed numerically in Sec. III.

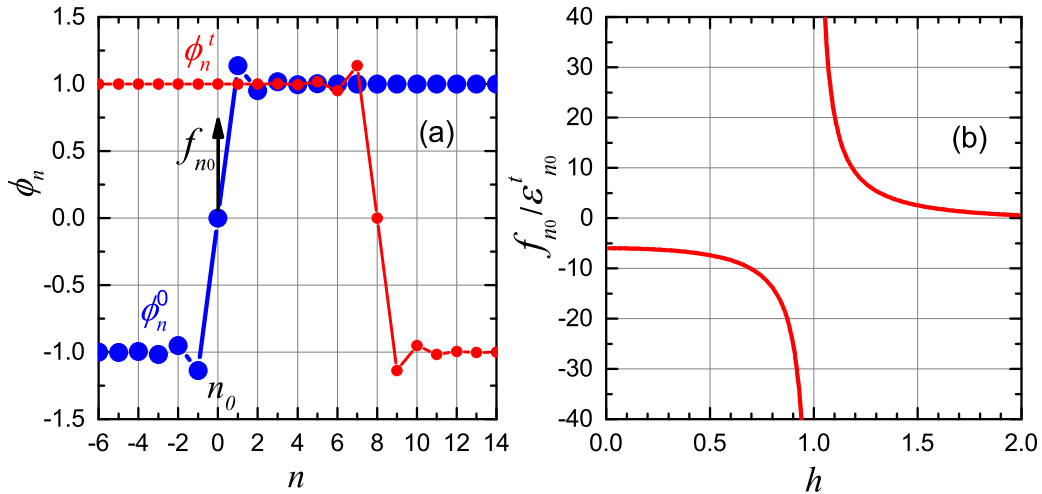


FIG. 2. (a) The setup of calculation of the force acting on the central particle of the on-site kink from the antikink's tail. The exact on-site static kink solution ϕ_n^0 (large circles) and the antikink (small circles) are shown. Here $h = 2$ and hence the kinks have oscillatory tails. The kink is located at $n = n_0 = 0$. (b) Normalized theoretically predicted force, $f_{n_0}/\epsilon_{n_0}^t$, acting on the central particle of the on-site kink from the antikink's tail as calculated from Eq. (19).

III. KINK-ANTI-KINK COLLISIONS

A. Simulation setup

The set of equations of motion (7) was integrated numerically using the Störmer method of the sixth order with the time step $\tau = 0.005$. The kink-antikink collisions were investigated in the chain having sufficiently large number of particles N , so that the radiation emitted by the colliding kinks does not reach the ends of the chain by the end of the simulation run. This way the effect of the radiation on the kink dynamics is avoided. Fixed boundary conditions were employed, $\phi_L = \phi_R = -1$, where ϕ_L and ϕ_R are the particles at the left and right ends of the chain, respectively (though the type of boundary conditions is not important for such sufficiently long chains).

The moving kink can be obtained by using the Goldstone translational mode e_1 , see Fig. 1(c). The initial conditions were formulated as follows. At $t = 0$ we set $\phi_n = \phi_n^0$, where ϕ_n^0 is the static kink solution, and at $t = \tau$ the Goldstone mode is added, $\phi_n = \phi_n^0 + \delta(e_1)_n$, with a small coefficient δ which defines the speed of the boosted kink. The eigenvector e_1 is assumed to be normalized, $\|e_1\| = 1$. The resulting kink velocity is measured numerically and it is called collision velocity v_c .

The obtained kink moving with the velocity v_c collides with its mirror image antikink having velocity $-v_c$ in the middle of the chain. The initial distance between the kink and antikink is taken sufficiently large for their exponential tails to not overlap.

B. Numerical results

Examples of the kink-antikink collisions are presented in Fig. 3: in (a)–(a'') for $h = 0.5$, in (b)–(b'') for $h = 0.9$, in (c)–(c'') for $h = 1.1$, and in (d)–(d'') for $h = 1.5$, by plotting the particles with the maximal energy. The collision velocity in each row increases from the left to the right.

It can be clearly inferred that the collisions are qualitatively different for $h < 1$ and $h > 1$, since the kink profiles are different in these two cases, see Eq. (16) and Fig. 1(a) for the kink tails, and the sign of the force acting between the kink and antikink changes at $h = 1$, as it was demonstrated in Sec. IID. Indeed, in line with the suggestive theoretical analysis of the previous section for $h < 1$ ($h > 1$) the kink and antikink attract (repel) each other.

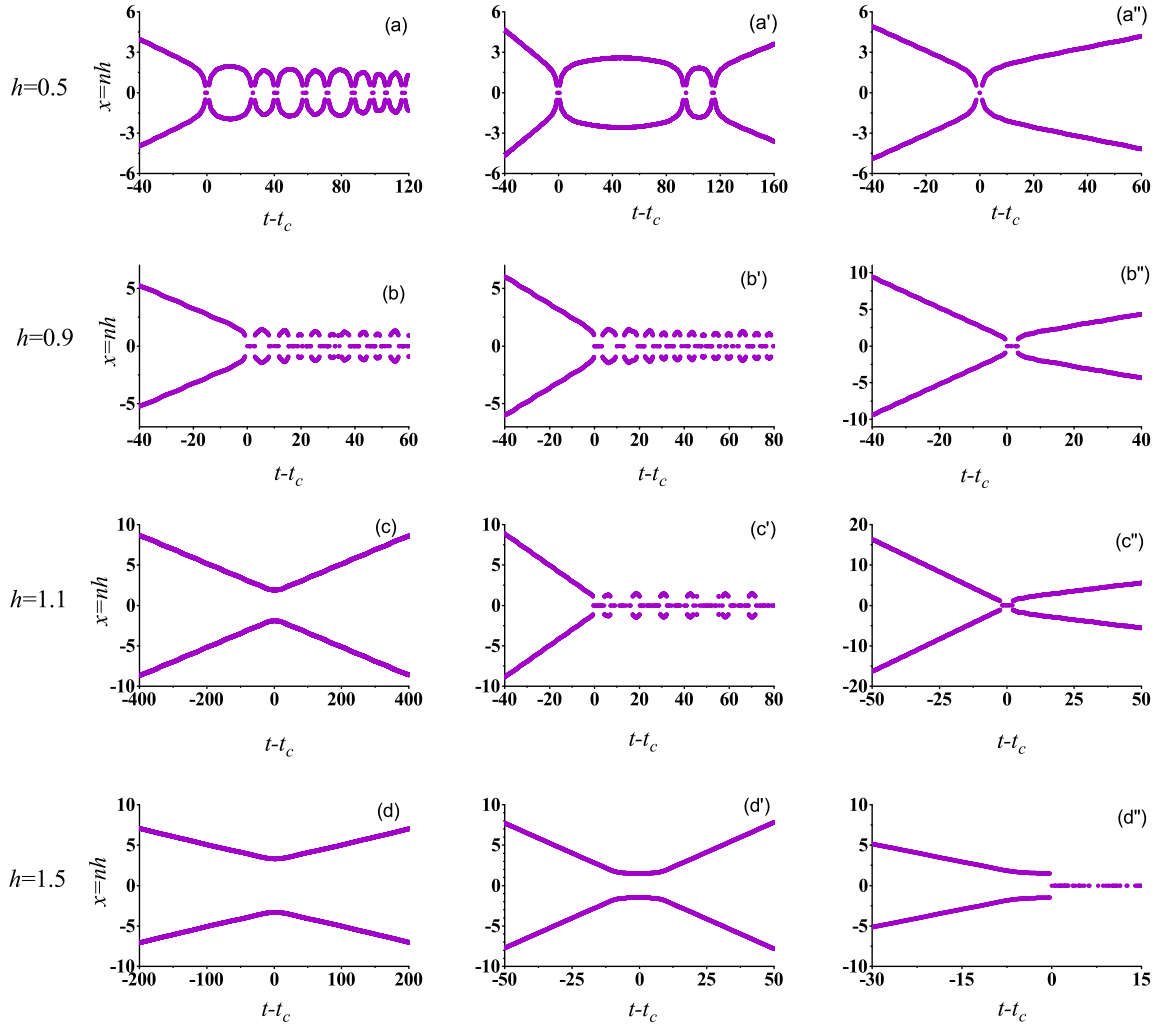


FIG. 3. Trajectories of colliding kinks and antikinks in the time-space plane for $h = 0.5$ in (a)-(a''), for $h = 0.9$ in (b)-(b''), for $h = 1.1$ in (c)-(c''), and for $h = 1.5$ in (d)-(d''), shown by plotting the particles with the maximal energy. The origin of the temporal coordinate is chosen at the collision time moment t_c . The collision velocity v_c increases in each row from the left to the right having the values: (a) 0.06062, (a') 0.08237, (a'') 0.09069; (b) 0.1, (b') 0.15, (b'') 0.2; (c) 0.01751, (c') 0.1958, (c'') 0.2501; (d) 0.01994, (d') 0.1481, (d'') 0.1486.

At $h < 1$ (two upper rows of Fig. 3) the kink and antikink attract each other as in the continuum case. In the first row the phonon band width is relatively large and it is small in the second row. Collisions are not elastic and a part of the energy of the kink and antikink related to their translational motion is converted into long-lived vibrational modes, while a

smaller portion of energy is radiated in the form of small-amplitude waves. If the collision velocity is above a threshold value v^* , the coherent structures pass through each other and continue their motion with a reduced velocity $v < v_c$, as exemplified in (a'') and (b''). Plots (a) and (a') show collisions with velocity $v_c < v^*$. Here the waves after the collision cannot overcome their mutual attraction and collide again. In (a) a bion is formed, which is a kink-antikink bound state. The bion's frequency is below the phonon band, $\omega_B < \omega_1 = 2$. From Eq. (13), for $h = 0.5$ the upper edge of the phonon band is $\omega_2 = 4$. This means that bion's higher harmonics are always within the phonon band, and thus the bion radiates its energy due to the relevant resonance mechanism. In (a'), we have a three-bounce collision after which the kinks separate and continue their motion with a velocity $v < v_c$. Such multi-bounce collisions with $v_c < v^*$ are possible because the energy stored by the kinks' internal modes can be transformed back into the energy of kinks' translational motion. This suggests that here we are still in a regime proximal to the continuum limit where such phenomenology is well-known to be prominent [24, 27, 28]. In (b) and (b') the collision velocity is also below v^* . However in this case the width of the phonon band is small and a discrete breather (DB) is formed with its frequency and all higher harmonics outside the phonon band. Thus, there is no mechanism for the breather to radiate its energy and it can be expected to persist over a long-time evolution.

At $h > 1$ the kink and antikink with oscillatory tails do not attract but repel each other. This is clearly seen in (c), (d) and (d'), where the collision velocity is below a threshold value v^{**} sufficient to overcome their repulsion. In (c'), (c'') and (d'') the collision velocity is above v^{**} and the kinks indeed collide. In (c'') they emerge after the collision with the velocity smaller than v_c . In (d''), as a result of the collision, a bion is produced with the main frequency within the relatively wide phonon band. The bion disappears after a few oscillations producing a burst of radiation (data not shown here).

On the other hand, in (c') the phonon band is narrow and a DB is formed with frequency $\omega_{DB} < \omega_2$, i.e., below the phonon band with all higher harmonics above the phonon band, hence the relevant waveform is expected to persist, in line with what is shown in the associated evolution dynamics.

Two critical velocities were defined above, v^* for $h < 1$ and v^{**} for $h > 1$. In Fig. 4 the critical velocities are plotted as functions of h . The critical velocity v^* has a minimum at $h = 0.6$; here, collisions are most elastic. v^* denotes the threshold here above which

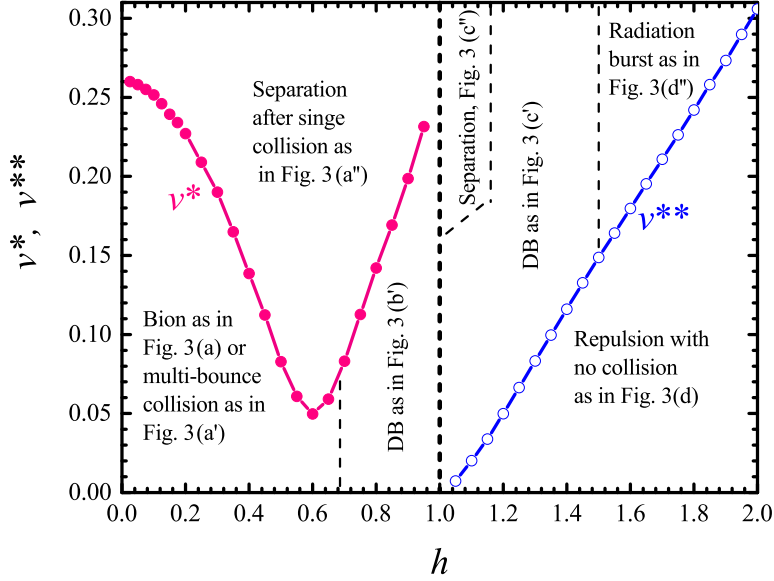


FIG. 4. Critical collision velocities v^* and v^{**} as the functions of h , for $h < 1$ and $h > 1$, respectively. For $v_c > v^*$ kink and antikink separate after the first collision, as shown in Fig. 3(a''). For $v_c < v^*$ and $h < 0.7$ they either create a bion, Fig. 3(a), or separate after a multi-bounce collision, Fig. 3(a'). For $v_c < v^*$ and $0.7 < h < 1$ a DB is formed, Fig. 3(b) or (b'). When $v_c > v^{**}$ the kink and antikink collide forming a DB ($1 < h < 1.5$, Fig. 3(c')) or a burst of radiation ($h > 1.5$, Fig. 3(d'')). For sufficiently large v_c and h close to 1 kink and antikink separate after first collision, Fig. 3(d''). For $v_c < v^{**}$ they repel each other, Fig. 3(c) or (d), or (d').

separation of the kink-antikink pair occurs after a single collision. The critical velocity v^{**} increases linearly with h . $v < v^{**}$ denotes the scenario of repulsion without interaction in this case of $h > 1$. Depending on h and the collision velocity, Fig. 4 is divided into parts where different collision scenarios are observed, as linked to the panels of Fig. 3.

More information on the effect of the collision velocity on the collision outcome is presented in Fig. 5. For instance, for $h = 0.5$ in the top panel of (a) the frequency of a bion formed when collision velocity is relatively small is shown by dots as a function of v_c . The circles show the frequency of the bion's second harmonic. Horizontal dashed lines show the borders of the phonon spectrum frequencies, ω_1 and ω_2 . It can be seen that the bion's frequency is always below the phonon spectrum but its second or third harmonic is within the spectrum. For $v_c > 0.08 = v^*$ the kink and antikink separate after the first collision. The

bottom panel shows the bion frequency as a function of its amplitude for all the cases where a bion was formed for $h = 1.2$ (left) and $h = 1.3$ (right). Similar results are presented in (b) for $h = 0.9$, but in this case not a bion but a DB is formed with the main frequency below the phonon band and all higher harmonics lie above the phonon band, hence suggesting the long time persistence of the structure.

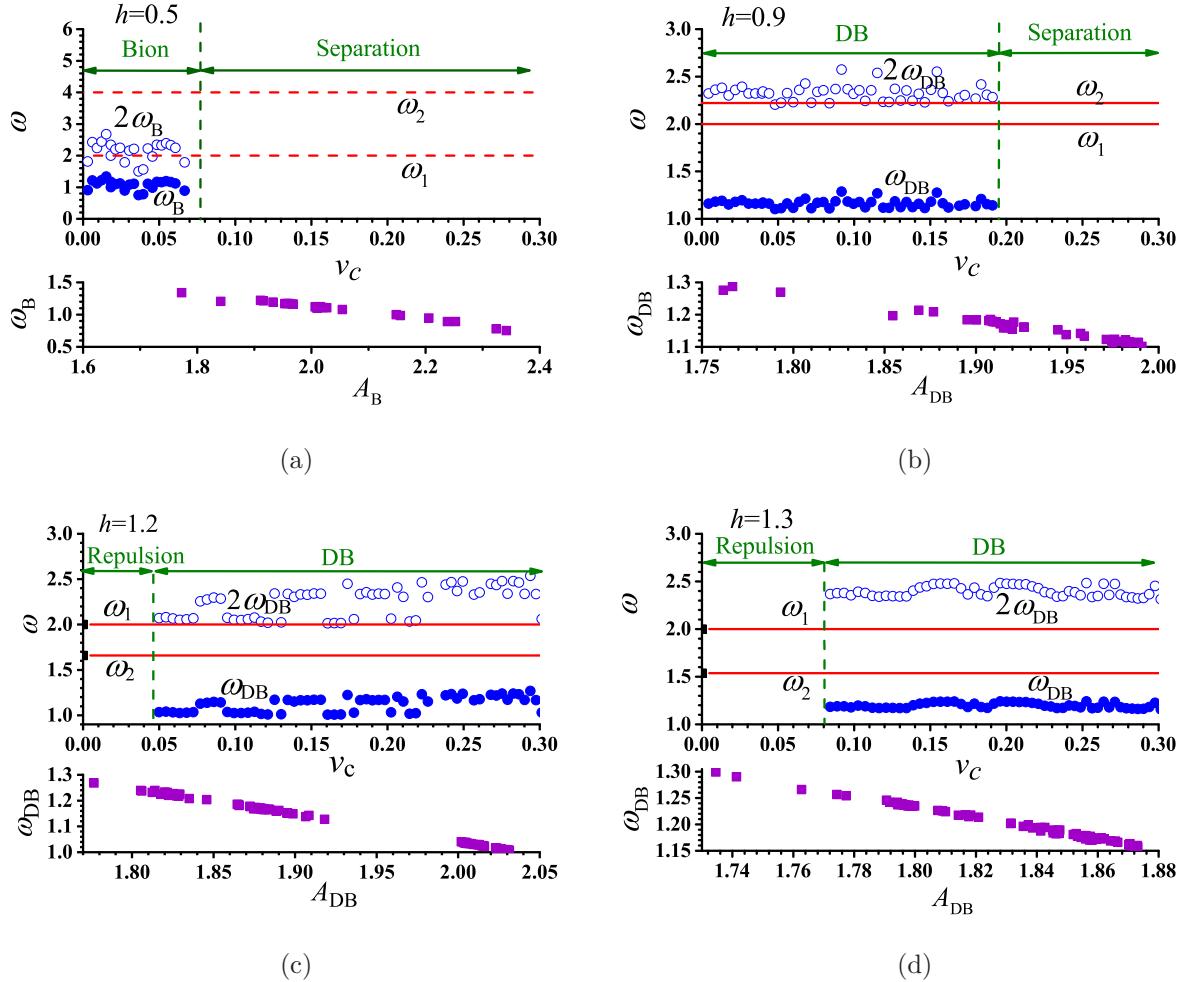


FIG. 5. Top panels: effect of the collision velocity v_c on the collision outcome for (a) $h = 0.5$, (b) $h = 0.9$, (c) $h = 1.2$, and (d) $h = 1.3$. Horizontal dashed lines show the borders of the phonon spectrum, ω_1 and ω_2 . Bion frequency ω_B , or DB frequency ω_{DB} , are shown by dots, and the second harmonics by circles. Bottom panels: (a) frequency of a bion formed in the collision with $v_c < 0.07$ as the function of its amplitude; (b)–(d) frequency of DB, formed as a result of collision with sufficiently large velocity as the function of its amplitude.

IV. CONCLUSIONS AND FUTURE WORKS

Kink-antikink collisions were analyzed numerically in the discrete ϕ^4 model, Eq. (7), which is free of the static Peierls–Nabarro potential. The lattice spacing h of order unity was considered, which corresponds to a high discreteness with the kink spanning only just a few lattice sites, see Fig. 1(a). Exact static kink solutions were derived iteratively from the two-point map (9) starting from any admissible initial value ϕ_n . The existence of a one-parameter set of static kinks positioned arbitrarily with respect to the lattice ensures the existence of the zero frequency Goldstone translational mode, see Fig. 1(c). The profile of this mode can be found by solving the eigenvalue problem for the equations of motion linearized near the static kink solution (11). The moving kink can be obtained with the help of the Goldstone mode as described in Sec. III A. Only symmetric collisions between the kink and its mirror image antikink moving with velocities v_c and $-v_c$, respectively, were addressed.

The borders of the phonon spectrum of the considered lattice, ω_1 and ω_2 , cross at $h = 1$, see Fig. 1(b). Around $h = 1$ spectrum width is small (and precisely at $h = 1$ it vanishes). Crossing of the phonon band edges changes the kink profile: for $h < 1$ kink’s tails are monotonic but for $h > 1$ they oscillate near the asymptotic states of ± 1 , as follows from Eq. (16) for the kink tails and as can be seen in Fig. 1(a). More importantly, for $h < 1$ kink and antikink are mutually attractive topological solitons, while for $h > 1$ they repel each other, as was shown in Sec. II D and in our collisional dynamics. The collision outcome is qualitatively different for attractive ($h < 1$) and repulsive ($h > 1$) kink and antikink, as summarized below.

For $h < 1$ collisions with a velocity $v_c > v^*$ result in separation of the kink and antikink after the first collision, see Fig. 3(a'') or (b''). The critical velocity v^* decreases with increasing h in the range $h < 0.6$ and increases for larger h , see Fig. 4. Collisions with a velocity smaller than v^* can result in either separation of the kink and antikink after a multi-bounce collision, see Fig. 3(a'), or in formation of an oscillatory mode. For $h < 0.7$, when the phonon band is wide, the oscillatory mode is a bion, see Fig. 3(a), with frequency below the phonon band and higher harmonics within the band, see the upper panel of Fig. 5(a). Due to the interaction with the phonons, the bion constantly radiates energy, its amplitude decreases and frequency increases, see lower panel of Fig. 5(a). For $0.7 < h < 1$ the phonon

band width is small and the oscillatory mode is a DB, see Fig. 3(a) or (b'), with the main frequency lying below the phonon band and all higher harmonics above the band as shown in the upper panel of Fig. 5(b). The DB does not interact with the phonon and has a very long lifetime.

For $h > 1$ the kink and antikink moving toward each other with a velocity $v_c < v^{**}$ cannot overcome the repulsion and they actually do not collide, see Fig. 3(c), or (d), or (d'). The critical velocity v^{**} increases linearly with increasing h , see Fig. 4. Collision with a velocity above v^{**} can result in either separation of the kink and antikink after single collision, see Fig. 3(c''), or in formation of a DB, see Fig. 3(c'), or in a burst of radiation producing a rapidly decaying bion, see Fig. 3(d''), where the radiation burst itself is not shown. A DB is formed for $1 < h < 1.5$ where the phonon band width is small. In this case the DB frequency is below the phonon band with all higher harmonics being above the band; see the upper panels of Fig. 5(c) and (d). An energy burst is produced for $h > 1.5$ when the colliding kink and antikink create an oscillatory mode with frequency inside a relatively wide phonon band. Such a mode radiates energy very quickly and it has a very short lifetime.

Note that when the colliding kink and antikink produce an oscillatory mode, the mode has frequency within the range from 0.8 to 1.3 in a wide range of h , see Fig. 5. In a forthcoming study properties of DBs will be addressed in detail regardless the mechanism of their generation (generated not only in kink-antikink collisions) in the whole range of possible frequencies. So far DBs have not been analyzed in the discrete systems free of the static Peierls–Nabarro potential. One of the most intriguing features here is the DB mobility: it is relevant to understand whether it is enhanced or not due to the absence of the static Peierls–Nabarro potential. Contrary to more standard models, the present scenario has the potential of mobile breathers even for regimes of high discreteness, a feature that is uncommon outside the realm of integrable models.

Another direction for the future studies is the analysis of kink collisions in the ϕ^6 and ϕ^8 models [30, 31, 34, 39, 60]. Interestingly, kinks in the ϕ^6 model are asymmetric and have short-range tails [30, 34, 60]. In the ϕ^8 and some other models kinks can have long-range tails with power-law decay [39, 56–59]. It would be interesting to study kink collisions in these models in the regime of high discreteness. In the work [61] two discrete ϕ^6 models free of the static Peierls–Nabarro potential have been derived. Generalizing such a derivation to ϕ^8 , ϕ^{10} and ϕ^{12} would enable the consideration of the intriguing interplay of discreteness of

long-range interactions. A discrete realm may be more straightforward of a place to consider such long-range interactions given that extended lattices would be easier to consider than the considerably more computationally expensive continuum analogues thereof.

The third natural continuation of this work is the analysis of the multi-bounce collisions and the related analysis of the kink's internal modes. As it can be seen from Fig. 1(b), in the case of small h there is only one kink's internal mode with the frequency $\omega \approx \sqrt{3}$, but for $h \sim 1$ the kink has more than one internal modes with frequencies below the phonon spectrum. This fact should affect the picture of multi-bounce collisions and this was indeed observed in our preliminary simulations.

ACKNOWLEDGMENTS

The work of the MEPHI group was supported by the MEPHI Academic Excellence Project (Contract No. 02.a03.21.0005, 27.08.2013). V.A.G. and S.V.D. acknowledge the support of the Russian Foundation for Basic Research, Grant No. 19-02-00971. S.V.D. also thanks the Tomsk State University competitiveness improvement programme. The work was partly supported by the State assignment of IMSP RAS. PGK gratefully acknowledges the hospitality of the Mathematical Institute of the University of Oxford and the support of the Leverhulme Trust during the final stages of this work. This material is based upon work supported by the US National Science Foundation under Grant DMS-1809074 (PGK).

-
- [1] R.K. Dodd, J.C. Eilbeck, J.D. Gibbon, H.C. Morris, *Solitons and Nonlinear Wave Equations*, Academic Press (London, 1982).
 - [2] O.M. Braun, Yu.S. Kivshar, *The Frenkel–Kontorova Model: Concepts, Methods, and Applications*, Springer-Verlag, Berlin 2004.
 - [3] P.G. Kevrekidis, J. Cuevas-Maraver, *A dynamical perspective on the ϕ^4 model: past, present and future*, Nonlinear Systems and Complexity (Springer Nature Switzerland 2019).
 - [4] J. Cuevas-Maraver, P.G. Kevrekidis, F. Williams (Eds.), *The sine-Gordon model and its applications: From pendula and Josephson Junctions to Gravity and High-Energy Physics*, Springer-Verlag, Heidelberg 2014.

- [5] Yu.S. Kivshar, D.K. Campbell, *Peierls–Nabarro potential barrier for highly localized nonlinear modes*, Phys. Rev. E **48**, 3077 (1993).
- [6] G.L. Alfimov, E.V. Medvedeva, D.E. Pelinovsky, *Wave Systems with an Infinite Number of Localized Traveling Waves*, Phys. Rev. Lett. **112**, 054103 (2014) [[arXiv:1309.0183](#)].
- [7] Ya. Zolotaryuk, I.O. Starodub, *Moving embedded solitons in the discrete double sine-Gordon equation*, In: Nonlinear Systems, Vol. 2, p. 315 (2018). Understanding Complex Systems. Springer, Cham.
- [8] D.J. Frantzeskakis, N.I. Karachalios, P.G. Kevrekidis, V. Koukoulouyannis, K. Vettas, *Dynamical transitions between equilibria in a dissipative Klein–Gordon lattice*, J. Math. Anal. Appl. **472**, 546 (2019) [[arXiv:1809.07995](#)].
- [9] S.V. Dmitriev, N.N. Medvedev, A.P. Chetverikov, K. Zhou, M.G. Velarde, *Highly Enhanced Transport by Supersonic N-Crowdions*, Phys. Status Solidi Rapid Res. Lett. **11**, 1700298 (2017).
- [10] R.I. Babicheva, I. Evazzade, E.A. Korznikova, I.A. Shepelev, K. Zhou, S.V. Dmitriev, *Low-energy channel for mass transfer in Pt crystal initiated by molecule impact*, Comput. Mater. Sci. **163**, 248 (2019).
- [11] A. Moradi Marjaneh, D. Saadatmand, I. Evazzade, R.I. Babicheva, E.G. Soboleva, N. Srikanth, K. Zhou, E.A. Korznikova, S.V. Dmitriev, *Mass transfer in the Frenkel–Kontorova chain initiated by molecule impact*, Phys. Rev. E **98**, 023003 (2018) [[arXiv:1805.07200](#)].
- [12] E.A. Korznikova, I.A. Shepelev, A.P. Chetverikov, S.V. Dmitriev, S.Yu. Fomin, K. Zhou, *Dynamics and Stability of Subsonic Crowdion Clusters in 2D Morse Crystal* J. Exp. Theor. Phys. **127**, 1009 (2018).
- [13] J.F.R. Archilla, Yu.A. Kosevich, N. Jimenez, V.J. Sanchez-Morcillo, L.M. Garcia-Raffi, *Ultradiscrete kinks with supersonic speed in a layered crystal with realistic potentials*, Phys. Rev. E **91** 022912 (2015) [[arXiv:1406.4085](#)].
- [14] T.D. Swinburne, S.L. Dudarev, S.P. Fitzgerald, M.R. Gilbert, A.P. Sutton, *Theory and simulation of the diffusion of kinks on dislocations in bcc metals*, Phys. Rev. B **87** 064108 (2013) [[arXiv:1210.8327](#)].
- [15] L. Huang, R. Wang, S. Wang, *A new reconstruction core of the 30° partial dislocation in silicon*, Philos. Mag. **99**, 347 (2019).
- [16] L. Huang, S. Wang, *A theoretical investigation of the glide dislocations in the sphalerite ZnS*, J. Appl. Phys. **124**, 175702 (2018).

- [17] F.J. Buijnsters, A. Fasolino, M.I. Katsnelson, *Motion of Domain Walls and the Dynamics of Kinks in the Magnetic Peierls Potential*, Phys. Rev. Lett. **113**, 217202 (2014) [[arXiv:1407.7754](#)].
- [18] M. Hwang, A.F. Arrieta, *Solitary waves in bistable lattices with stiffness grading: Augmenting propagation control*, Phys. Rev. E **98**, 042205 (2018).
- [19] Yu.A. Kosevich, *Charged ultradiscrete supersonic kinks and discrete breathers in nonlinear molecular chains with realistic interatomic potentials and electron-phonon interactions*, J. Phys.: Conf. Ser. **833**, 012021 (2017).
- [20] S. Flach, A.V. Gorbach, *Discrete breathers — Advances in theory and applications*, Phys. Rep. **467**, 1 (2008).
- [21] P.J. Martinez, L.M. Floria, F. Falo, J.J. Mazo, *Intrinsically localized chaos in discrete nonlinear extended systems*, Europhys. Lett. **45**, 444 (1999) [[arXiv:chao-dyn/9901030](#)].
- [22] D.K. Campbell, J.F. Schonfeld, C.A. Wingate, *Resonance structure in kink-antikink interactions in φ^4 theory*, Physica D **9**, 1 (1983).
- [23] D.K. Campbell, M. Peyrard, *Solitary wave collisions revisited*, Physica D **18**, 47 (1986).
- [24] P. Anninos, S. Oliveira, R.A. Matzner, *Fractal structure in the scalar $\lambda(\varphi^2 - 1)^2$ theory*, Phys. Rev. D **44**, 1147 (1991).
- [25] V.A. Gani, A.E. Kudryavtsev, *Kink-antikink interactions in the double sine-Gordon equation and the problem of resonance frequencies*, Phys. Rev. E **60**, 3305 (1999) [[cond-mat/9809015](#)].
- [26] S.V. Dmitriev, Yu.S. Kivshar, T. Shigenari, *Fractal structures and multiparticle effects in soliton scattering*, Phys. Rev. E **64**, 056613 (2001).
- [27] R.H. Goodman, R. Haberman, *Kink-Antikink Collisions in the ϕ^4 Equation: The n -Bounce Resonance and the Separatrix Map*, SIAM J. Appl. Dyn. Syst. **4**, 1195 (2005).
- [28] R.H. Goodman, R. Haberman, *Chaotic Scattering and the n -Bounce Resonance in Solitary-Wave Interactions*, Phys. Rev. Lett. **98**, 104103 (2007) [[arXiv:nlin/0702048](#)].
- [29] S.V. Dmitriev, P.G. Kevrekidis, Yu.S. Kivshar, *Radiationless energy exchange in three-soliton collisions*, Phys. Rev. E **78**, 046604 (2008) [[arXiv:0806.1152](#)].
- [30] V.A. Gani, A.E. Kudryavtsev, M.A. Lizunova, *Kink interactions in the (1+1)-dimensional φ^6 model*, Phys. Rev. D **89**, 125009 (2014) [[arXiv:1402.5903](#)].
- [31] V.A. Gani, V. Lensky, M.A. Lizunova, *Kink excitation spectra in the (1+1)-dimensional φ^8 model*, JHEP **08**, 147 (2015) [[arXiv:1506.02313](#)].

- [32] E.G. Ekomasov, A.M. Gumerov, R.R. Murtazin, *Interaction of sine-Gordon solitons in the model with attracting impurities*, Math. Meth. Appl. Sci. **40**, 6178 (2017).
- [33] A. Moradi Marjaneh, D. Saadatmand, K. Zhou, S.V. Dmitriev, M.E. Zomorrodian, *High energy density in the collision of N kinks in the ϕ^4 model*, Comm. Nonlinear Sci. Numer. Simulat. **49**, 30 (2017) [[arXiv:1605.09767](#)].
- [34] A. Moradi Marjaneh, V.A. Gani, D. Saadatmand, S.V. Dmitriev, K. Javidan, *Multi-kink collisions in the ϕ^6 model*, JHEP **07**, 028 (2017) [[arXiv:1704.08353](#)].
- [35] A. Moradi Marjaneh, A. Askari, D. Saadatmand, S.V. Dmitriev, *Extreme values of elastic strain and energy in sine-Gordon multi-kink collisions*, Eur. Phys. J. B **91**, 22 (2018) [[arXiv:1710.10159](#)].
- [36] D. Bazeia, E. Belendryasova, V.A. Gani, *Scattering of kinks of the sinh-deformed φ^4 model*, Eur. Phys. J. C **78**, 340 (2018) [[arXiv:1710.04993](#)].
- [37] V.A. Gani, A. Moradi Marjaneh, A. Askari, E. Belendryasova, D. Saadatmand, *Scattering of the double sine-Gordon kinks*, Eur. Phys. J. C **78**, 345 (2018) [[arXiv:1711.01918](#)].
- [38] V.A. Gani, A. Moradi Marjaneh, D. Saadatmand, *Multi-kink scattering in the double sine-Gordon model*, Eur. Phys. J. C **79**, 620 (2019) [[arXiv:1901.07966](#)].
- [39] E. Belendryasova, V.A. Gani, *Scattering of the φ^8 kinks with power-law asymptotics*, Comm. Nonlinear Sci. Numer. Simulat. **67**, 414 (2019) [[arXiv:1708.00403](#)].
- [40] O.M. Braun, Yu.S. Kivshar, M. Peyrard, *Kink's internal modes in the Frenkel–Kontorova model*, Phys. Rev. E **56**, 6050 (1997).
- [41] I.V. Barashenkov, O.F. Oxtoby, D.E. Pelinovsky, *Translationally invariant discrete kinks from one-dimensional maps*, Phys. Rev. E **72**, 035602 (2005) [[arXiv:nlin/0506007](#)].
- [42] J.M. Speight, *A discrete ϕ^4 system without a Peierls–Nabarro barrier*, Nonlinearity **10**, 1615 (1997) [[arXiv:patt-sol/9703005](#)].
- [43] J.M. Speight, *Topological discrete kinks*, Nonlinearity **12**, 1373 (1999) [[arXiv:hep-th/9812064](#)].
- [44] P.G. Kevrekidis, *On a class of discretizations of Hamiltonian nonlinear partial differential equations*, Physica D **183**, 68 (2003).
- [45] P.G. Kevrekidis, A. Khare, A. Saxena, I. Bena, A.R. Bishop, *Asymptotic calculation of discrete non-linear wave interactions*, Math. Comp. Simul. **74**, 405 (2007).

- [46] S.V. Dmitriev, P.G. Kevrekidis, N. Yoshikawa, *Standard nearest-neighbour discretizations of Klein–Gordon models cannot preserve both energy and linear momentum*, J. Phys. A: Math. Gen. **39**, 7217 (2006) [[arXiv:nlin/0506002](#)].
- [47] S.V. Dmitriev, P.G. Kevrekidis, N. Yoshikawa, *Discrete Klein–Gordon models with static kinks free of the Peierls–Nabarro potential*, J. Phys. A: Math. Gen. **38**, 7617 (2005) [[arXiv:nlin/0506001](#)].
- [48] F. Cooper, A. Khare, B. Mihaila, A. Saxena, *Exact solitary wave solutions for a discrete $\lambda\phi^4$ field theory in 1 + 1 dimensions*, Phys. Rev. E **72**, 036605 (2005) [[arXiv:nlin/0502054](#)].
- [49] J.M. Speight, Y. Zolotaryuk, *Kinks in dipole chains*, Nonlinearity **19**, 1365 (2006) [[arXiv:nlin/0509047](#)].
- [50] S.V. Dmitriev, P.G. Kevrekidis, A. Khare, A. Saxena, *Exact static solutions to a translationally invariant discrete ϕ^4 model*, J. Phys. A: Math. Theor. **40**, 6267 (2007) [[arXiv:nlin/0703043](#)].
- [51] A. Khare, S.V. Dmitriev, A. Saxena, *Exact static solutions of a generalized discrete ϕ^4 model including short-periodic solutions*, J. Phys. A: Math. Theor. **42**, 145204 (2009) [[arXiv:0710.1460](#)].
- [52] C.M. Bender, A. Tovbis, *Continuum limit of lattice approximation schemes*, J. Math. Phys. **38**, 3700 (1997).
- [53] S.V. Dmitriev, A. Khare, P.G. Kevrekidis, A. Saxena, L. Hadzievski, *High-speed kinks in a generalized discrete ϕ^4 model*, Phys. Rev. E **77**, 056603 (2008) [[arXiv:0802.2375](#)].
- [54] I. Roy, S.V. Dmitriev, P.G. Kevrekidis, A. Saxena, *Comparative study of different discretizations of the ϕ^4 model*, Phys. Rev. E **76**, 026601 (2007) [[arXiv:nlin/0608046](#)].
- [55] D. Leykam, A. Andreanov, S. Flach, *Artificial flat band systems: from lattice models to experiments*, Adv. Phys.: X **3**, 1473052 (2018) [[arXiv:1801.09378](#)].
- [56] I.C. Christov, R.J. Decker, A. Demirkaya, V.A. Gani, P.G. Kevrekidis, R.V. Radomskiy, *Long-range interactions of kinks*, Phys. Rev. D **99**, 016010 (2019) [[arXiv:1810.03590](#)].
- [57] I.C. Christov, R.J. Decker, A. Demirkaya, V.A. Gani, P.G. Kevrekidis, A. Khare, A. Saxena, *Kink-kink and kink-antikink interactions with long-range tails*, Phys. Rev. Lett. **122**, 171601 (2019) [[arXiv:1811.07872](#)].
- [58] N.S. Manton, *Forces between kinks and antikinks with long-range tails*, J. Phys. A: Math. Theor. **52**, 065401 (2019) [[arXiv:1810.03557](#)].

- [59] A. Khare and A. Saxena, *Family of potentials with power law kink tails*, J. Phys. A: Math. Theor. **52**, 365401 (2019) [[arXiv:1810.12907](#)].
- [60] A. Demirkaya, R. Decker, P.G. Kevrekidis, I.C. Christov, A. Saxena, *Kink dynamics in a parametric ϕ^6 system: a model with controllably many internal modes*, JHEP **12**, 071 (2017) [[arXiv:1706.01193](#)].
- [61] Zh.G. Rakhmatullina, P.G. Kevrekidis, S.V. Dmitriev, *Non-symmetric kinks in Klein–Gordon chains free of the Peierls–Nabarro potential*, IOP Conf. Ser.: Mater. Sci. Eng. **447**, 012057 (2018).